COMPDYN 2015
5th ECCOMAS Thematic Conference on
Computational Methods in Structural Dynamics and Earthquake Engineering
M. Papadrakakis, V. Papadopoulos, V. Plevris (eds.)
Crete Island, Greece, 25–27 May 2015

CLASS A PREDICTION FOR SEISMIC CENTRIFUGE MODELING OF MULTI-BLOCK QUAY-WALL: UNDRAINED (PLAXIS) VERSUS COUPLED (FLAC) EFFECTIVE STRESS ANALYSIS

Panagiota Tasiopoulou[1], Nikos Gerolymos[2], and George Gazetas[3]

[1] National Technical University of Athens, Greece
9, Iroon Polytechniou Str., Polytechnic Campus. Zografos P.C 15780
e-mail: ptasiopoulou@gmail.com

[2] National Technical University of Athens, Greece
9, Iroon Polytechniou Str., Polytechnic Campus. Zografos P.C 15780
gerolymos@gmail.com

[3] National Technical University of Athens, Greece
9, Iroon Polytechniou Str., Polytechnic Campus. Zografos P.C 15780
gazetas@ath.forthnet.gr

Keywords: quay-wall, seismic effective stress analysis, coupled flow dynamic response, FLAC, PLAXIS.

Abstract. *Effective stress analyses are conducted aiming to provide Class A predictions for a seismic centrifuge test of a multi-block gravity quay-wall. Two different codes are used: i) the finite difference code FLAC 2D (coupled effective- stress analysis) and ii) the finite element code, PLAXIS 2D (undrained effective-stress analysis). Two versions of the original UBCSAND constitutive model, implemented in each code, are used after meticulous calibration in order to reproduce equivalent liquefaction resistance curves. Apart from predicting the experimental response, the study aims at performing a comparison between the two codes widely-used in practice.*

1 INTRODUCTION

The latest advances in port and maritime industry have redefined the role of harbor facilities in the economy. Ports are nowadays multipurpose lifeline facilities that function as embarkation, storage and maintenance facilities for the transportation of cargo and passengers. Waterfront structures form the core of nearly all harbor facilities (be it commercial, industrial, or simply passenger terminals). Therefore maintaining their integrity (as well as a minimum serviceability threshold) during seismic events, constitutes a necessity for the sustainability pf the facility as a whole, since most of the components comprising any waterfront plant (e.g. pipelines, cranes, storage tanks etc.) are either founded, or directly dependent, upon them.

Gravity quay wall structures have repeatedly suffered substantial outward displacement and rotation even when subjected to moderate earthquake shaking. (e.g. [1]-[7]). The most astonishing case study comes from the port of Kobe, where during the 1995 earthquake, wall displacements reached as much as 5 m [8]. Yet, even during the mild Lefkada (Greece) earthquake of 2003 (Ms = 6.4) most of the coastal structures sustained relatively large displacements up to 25 cm. An even more recent example is the damage of the Lixouri harbour quay wall in the two 2014 Cephalonia (Greece) earthquakes, despite the relatively small magnitude (Ms ≈ 6) of the events.

The dynamic response of gravity quay walls is strongly affected by non-linear soil behaviour. Development of excess pore pressures and accumulation of shear and volumetric strains both at the retained and the foundation soil, produces shear strength degradation which may be accompanied by liquefaction. The above phenomena are further complicated when accounting for soil-structure interaction. The strong rocking of quay walls (due only to their inertial forces), when founded on a compliant foundation soil in combination with the one-sided action of earth pressures leads to the accumulation of horizontal displacement and rotation towards the seaside. Evidently, the deformation modes that synthesize the response of the quay wall at large displacements and near failure conditions cannot be realistically assessed by conventional design procedures. The use of suitable constitutive soil models [22] that balance simplicity and effectiveness in conjunction with powerful numerical techniques is a key-step for a successful prediction.

In this paper, effective stress numerical analyses are conducted aiming to provide Class A predictions for a seismic centrifuge test of a multi-block gravity quay-wall, replica of a typical wall at Piraeus port in Greece. The centrifuge testing was conducted at University of Dundee and the experimental measurements will be published by [9]. Two different codes are used: i) finite difference code, FLAC 2D [10] and ii) finite element code, PLAXIS 2D. Two different versions of the original elasto-plastic effective stress constitutive model [11]-[12], UBCSAND, have been implemented in each code: i) UBCSAND-904aR for FLAC [13] and ii) UBC3D-PLM for PLAXIS [14]. These versions are calibrated appropriately in an attempt to achieve equivalence in their predictions of liquefaction resistance stress ratios for the same number of loading cycles under undrained conditions. The goal of this study is twofold: a) to predict of the experimental response and b) to compare the computed response by two codes widely-used in practice, FLAC (coupled effective- stress analysis) and PLAXIS (undrained effective-stress analysis).

2 SEISMIC CENTRIFUGE MODELING

A dynamic centrifuge model test was conducted at the University of Dundee centrifuge facility is examined. The model used a fine quartz based silica sand (HST95) and simulated the response of a multi-block gravity quay wall made of aluminium alloy, as a replica of a typical

wall at Piraeus port in Greece. The sand bed was formed into an ESB (equivalent shear beam) model container by carrying out air pluviation at a relative density of D_r = 80%. It was then saturated with water and subjected to an acceleration field of 60g. A sketch of the experimental setup (including the instrumentation layout) is illustrated in figure 1. While in flight, a sequence of actual ground-acceleration records were applied at the base of the model as input motion. However, only numerical results for the first acceleration time history (a record from the M_L = 5.9 L' Aquila 2009 earthquake, shown in Figure 2) are presented as class A predictions. Details on the experimental procedure and measurements will be published by [9].

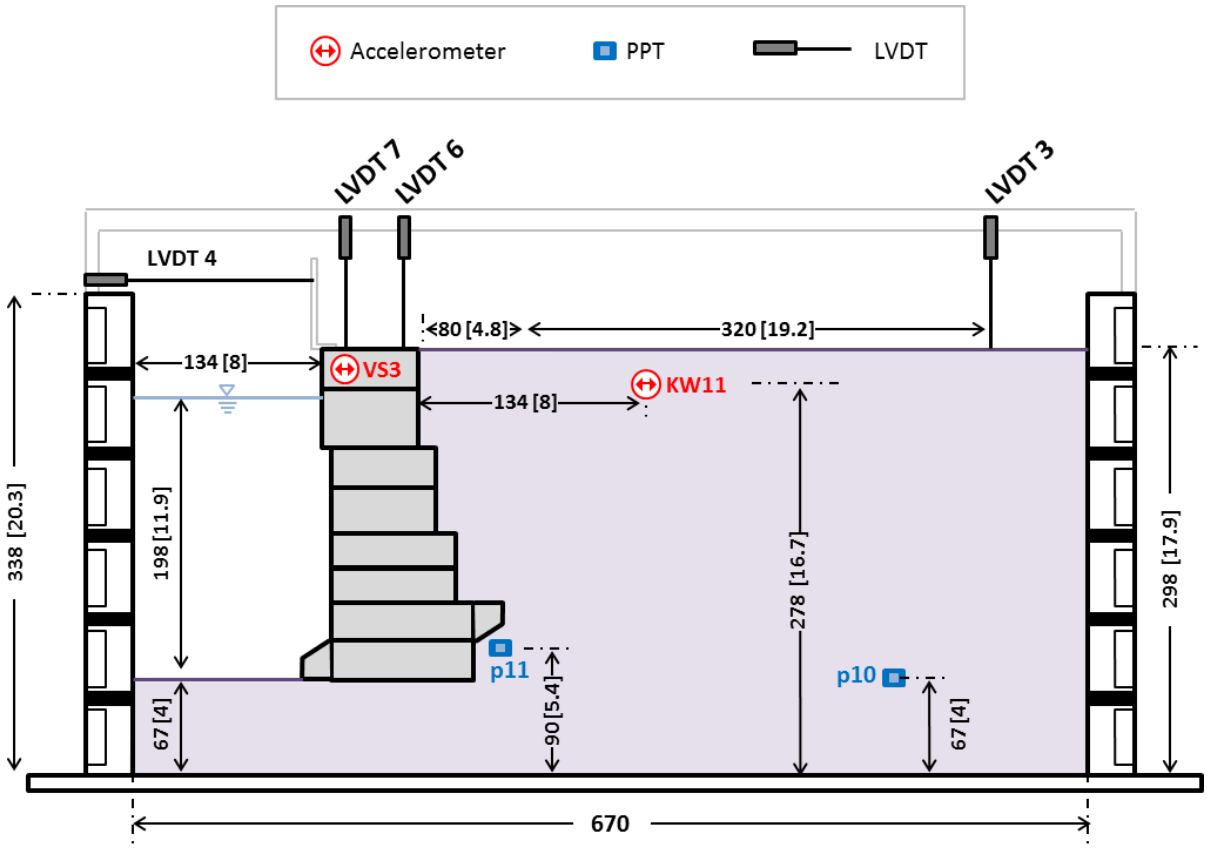

Figure 1. Centrifuge model setup and instrument locations for Class A prediction.

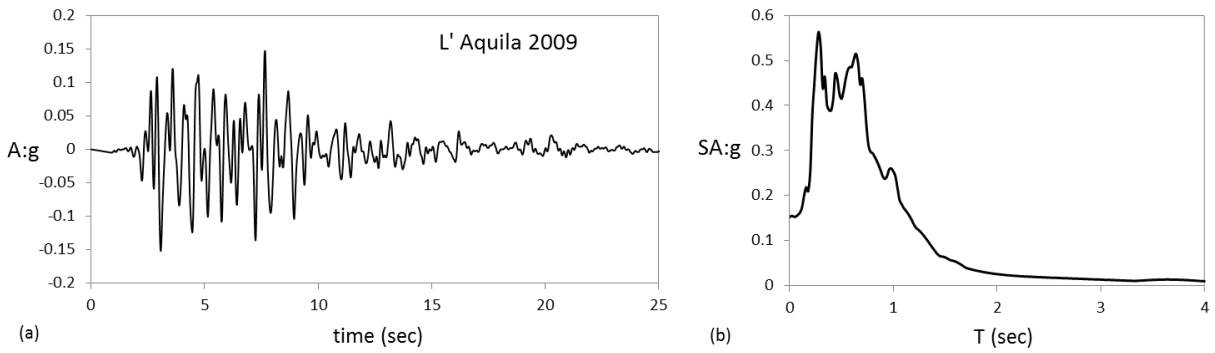

Figure 2. Base input motion: Acceleration time history and corresponding spectrum

3 NUMERICAL MODELING

Numerical effective stress analysis of a section of the centrifuge model is performed in prototype scale with both finite difference code FLAC and finite element code PLAXIS. The analysis is conducted taking into account for material (in the soil) and geometric (interface) nonlinearities. The aluminium alloy frames and rubber spacing layers of the ESB model container were also modelled in detail, assuming elastic behaviour. Prescribed displacements were imposed on the horizontal boundaries of each frame prohibiting their movement in the vertical direction, and kinematic constraints were assigned to the external and internal vertical edges of the model allowing it to move as a laminar box ([14]- [17]).

The contact conditions between the blocks of the quay wall as well as between the quay wall and the adjacent soil were modelled with special interface elements allowing for slippage and gapping via a Coulomb frictional law. Special interface elements were also placed along the inner edges of the ESB model container. The friction interface angles were assumed equal to 18^o between the blocks of the quay wall, 10^o and 14^o at the back and at the base of the wall, respectively, and 10^o for the inner vertical edges of the container. The waterfront was simulated through hydrostatic pressures applied to the front side of the wall, as well as the seabed. To avoid spurious oscillations at very small deformations and for high frequency components of motion, Rayleigh damping was also introduced into the model, accounting for equivalent hysteretic damping values between 1.5% and 3% in the range of 0.2 Hz and 2 Hz. The initial horizontal effective stresses were set to 0.5 times the vertical effective stresses. The input motion in prototype scale, in Figure 2, was applied to the base of the numerical models.

3.1 COUPLED ANALYSIS - FLAC

The finite difference mesh of the model, portrayed in Figure 3, involves a grid spacing of 0.5 m x 0.5 m. FLAC allows for coupled flow dynamic analysis, accounting for interaction of the poro mechanical soil properties. The coefficient of hydraulic permeability was estimated to $k = 3 \times 10^{-4}$ m/s (in prototype scale) and assumed to be constant throughout the analysis.

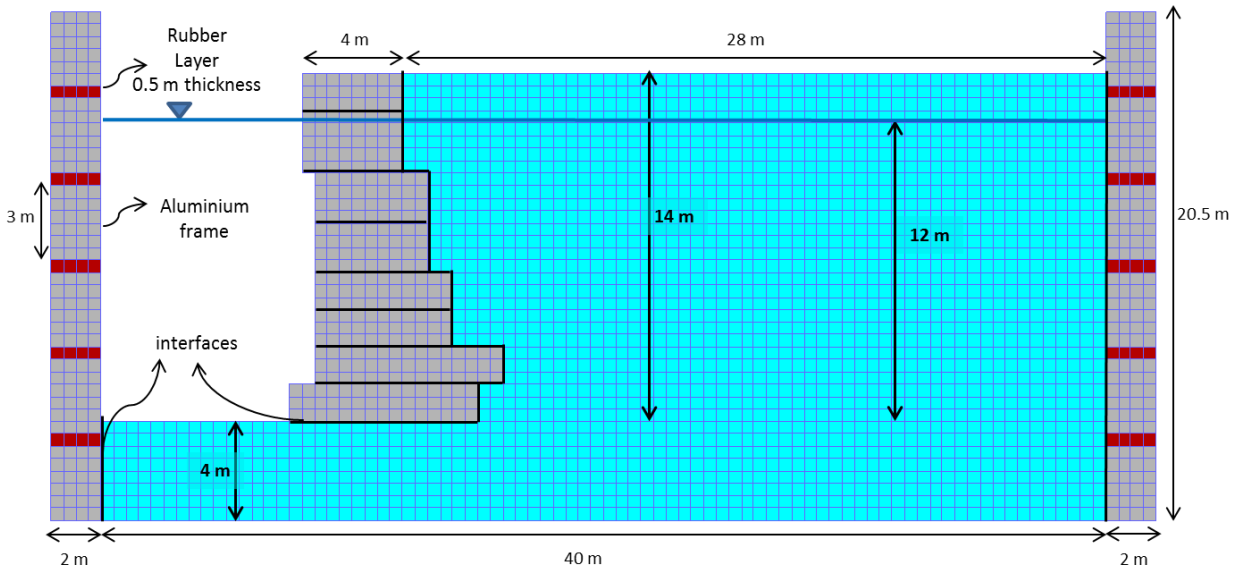

Figure 3. Numerical model in FLAC.

3.2 UNDRAINED ANALYSIS - PLAXIS

Undrained effective stress analysis was conducted with finite element code PLAXIS 2D AE. Both the quay wall and the soil are modelled with 15-node triangular plane strain elements, elastic for the former and nonlinear for the latter (3130 elements in total). The finite element mesh is shown in Figure 4.

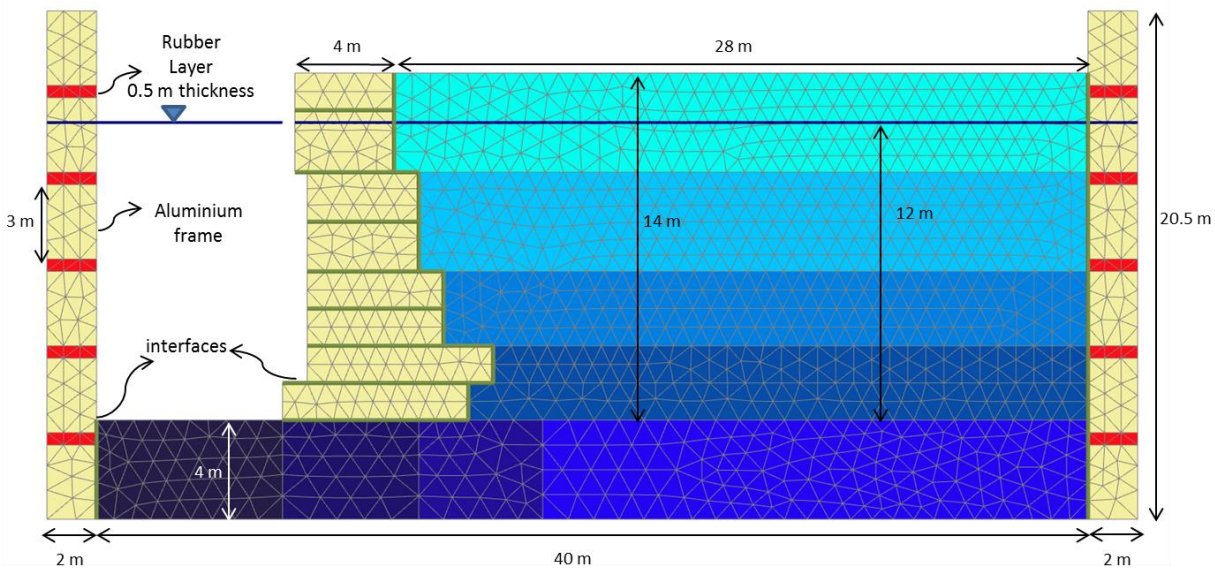

Figure 4. The finite element model (PLAXIS)

4 CONSTITUTIVE MODEL

Cyclic soil behaviour is described through an elasto-plastic effective stress constitutive model, UBCSAND, originally developed at University of British Columbia by [11] and [12]. It involves two yield surfaces (a primary and a secondary one) of the Mohr-Coulomb type. The primary surface evolves according to an isotropic hardening law while a simplified kinematic hardening rule is used for the second yield surface. The elastic response is described by the elastic shear and bulk moduli given by:

$$G^e = k_G^e \cdot p_a \cdot \left(p / p_a \right)^{ne} \tag{1}$$

$$B^e = k_B^e \cdot p_a \cdot \left(p / p_a \right)^{me} \tag{2}$$

in which k_G^e and k_B^e are the elastic shear and bulk numbers in respect, p_a is the reference stress, p is the mean effective stress and ne, me are exponents for stress dependency. The plastic shear modulus is given by:

$$G^p = G_i^p \left(1 - \frac{\eta}{\eta_f} R_f \right)^2 \tag{3}$$

in which G_i^p component variates for primary, secondary and post-dilation loading, η is the current stress ratio, η_f is the stress ratio at failure, equal to $sin\left(\varphi_p\right)$, φ_p being the peak friction angle and R_f is a failure ratio that truncates hyperbolic curve. The plastic flow rule is non-associated and is based on the Drucker-Prager's law and Rowe's stress dilatancy hypothesis:

$$d\varepsilon_v^p = \left(sin\left(\varphi_{cv}\right) - \eta\right) d\gamma^p \tag{4}$$

where φ_{cv} is the phase transformation friction angle.

Different versions and extensions of the model, based on the above-described framework, have been developed by various researchers. The most widely-used ones, are those implemented in finite difference code, FLAC and finite element code, PLAXIS, such as UBCSAND-904aR [13] and UBC3D-PLM [14], respectively. One of the most significant divergences of the two versions, when performing seismic effective stress analysis, lies on their approach on the stiffness degradation of the secondary plastic shear modulus, which practically controls the number of loading cycles to cause liquefaction.

4.1 UBCSAND 904aR in FLAC

In this version of the model, G_i^p component has the following form:

$$G_i^p = k_G^p \cdot \frac{p_a}{p} \cdot \left(\frac{p}{p_a}\right)^{np} \cdot f\left(hfac_1, hfac_2, n_{cyc} \ldots\right) \tag{5}$$

where k_G^p is the plastic shear modulus number, np is a constant, $hfac_1$ is a factor controlling the number of cycles to trigger liquefaction and $hfac_2$ is a factor refining the shape of pore water pressure rise with cycles, n_{cyc} is the number of loading cycles etc. Obviously, the decisive parameter to define the liquefaction resistance versus number of loading cycles is $hfac_1$. The smaller the value of $hfac_1$, the greater the excess pore water pressure development and the lesser the liquefaction resistance.

4.2 UBC3D-PLM in PLAXIS

In this version, G_i^p component is described as:

$$G_i^p = k_G^p \cdot \frac{p_a}{p} \cdot \left(\frac{p}{p_a}\right)^{np} \cdot f\left(fac_{hard}, n_{cyc,\ldots}\right) \tag{6}$$

in whih fac_{hard} affects the number of cycles for liquefaction occurrence. This parameter has the same trend as $hfac_1$, in the previous version; thus, lower values lead to lesser number of cycles required to cause liquefaction.

4.3 Calibration Methodology

[13] proposed a set of equations for the calibration of the UBCSAND model parameters, with the corrected SPT value $(N_1)_{60}$ being the sole variable. The calibration procedure aimed

at matching the cyclic resistance ratio indicated by the NCEER/NSF curve for a given corrected SPT blow count to induce liquefaction at 15 uniform loading cycles. In order to apply this methodology to our study, the empirical correlation between $(N_1)_{60}$ and relative density, D_r , proposed by [18] was used:

$$(N_1)_{60} \simeq 46 (D_r)^2 \tag{7}$$

Thus, applying the methodology by Beaty and Byrne (2011) for both versions of UBCSAND , while assuming that φ_p = 42°, as indicated by experiments of HST95 Silica sand for $D_r = 80\%$, the values of the common model parameters were derived, as shown in Table 1. Then, the different parameters of the two versions, $hfac_1$ for UBCSAND-904aR and fac_{hard} for UBC3D-PLM, were calibrated based on experimental liquefaction resistance curves for various sands with $D_r = 80\%$ ([19]-[21]), as shown in Figure 5. The goal of this calibration process was to achieve equivalence of the two versions in predicting the number of loading cycles to cause liquefaction under specific cyclic stress ratios. Finally, in order to incorporate stress dependency, or the so-called Kσ effects, the model parameters, $hfac_1$ and fac_{hard}, are given as functions of the vertical effective stress, as illustrated in Figures 6 and 7. Representative results of computed response for both versions are shown in figure 8, for CSR = 0.3, initial effective stress σ'_{v0} = 100 kPa and lateral earth pressure coefficient at rest K_0 = 0.5.

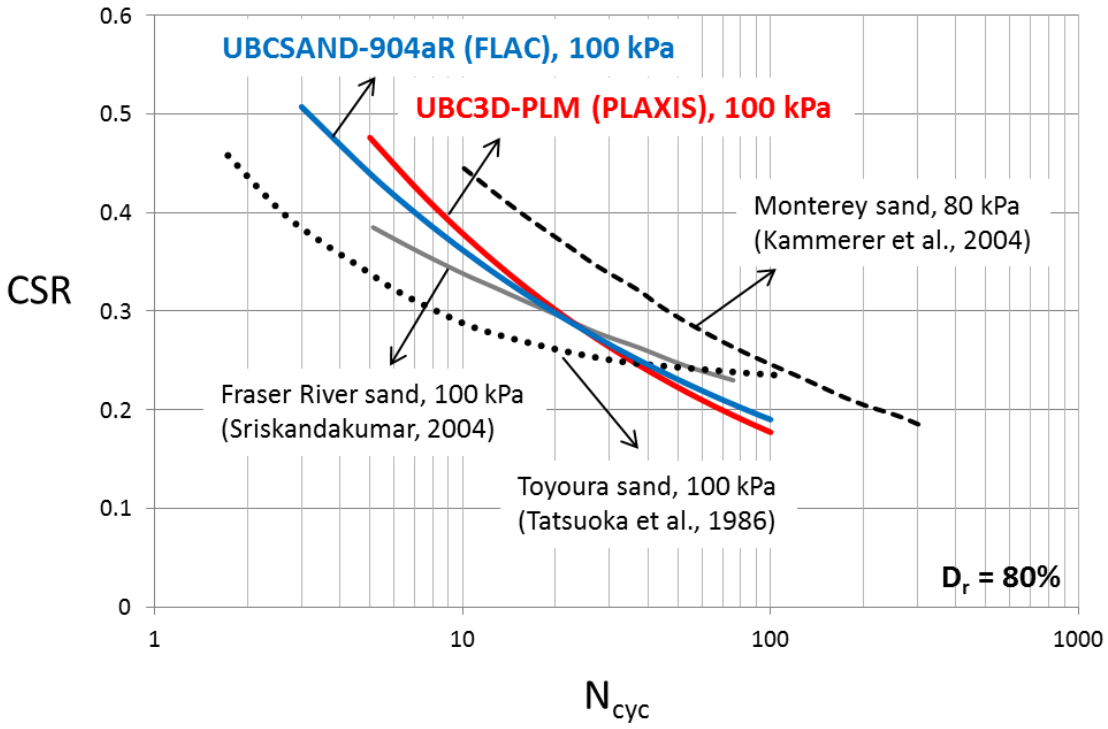

Figure 5. Comparison between predicted and experimental liquefaction resistance curves in undrained cyclic simple shear testing for D_r = 80%.

Parameters	Unit	Description	UBC3D-PLM (PLAXIS)	UBCSAND-904aR (FLAC)
φ_p	(deg)	Peak friction angle	42	42
φ_{cv}	(deg)	Phase transformation friction angle	36.1	36.1
k^e_B	-	Elastic bulk modulus number	937	937
K^e_G	-	Elastic shear modulus number	1338.6	1338.6
k^p_G	-	Plastic shear modulus number	3580.5	3580.5
me	-	Exponent for stress dependency of elastic bulk modulus	0.5	0.5
ne	-	Exponent for stress dependency of elastic shear modulus	0.5	0.5
np	-	Power for stress dependency of plastic shear modulus	0.4	0.4
R_f	-	Failure ratio	0.662	0.662
p_a	(kPa)	Reference stress	100	100
fac_{hard}	-	Fitting parameter to adjust number of cycles to liquefaction	see Fig. 7	N/A
fac_{post}	-	Fitting parameter to adjust post- dilation behaviour	0.01	N/A
$hfac_1$	-	Fitting parameter to adjust number of cycles to liquefaction	N/A	see Fig. 6
$hfac_2$	-	Fitting parameter to refine shape of pore pressure rise with cycles	N/A	1
$(N_1)_{60}$	-	Corrected SPT blow counts	29.4	29.4

Table 1. Constitutive model parameters for UBC3D-PML (PLAXIS) and UBCSAND-904aR (FLAC).

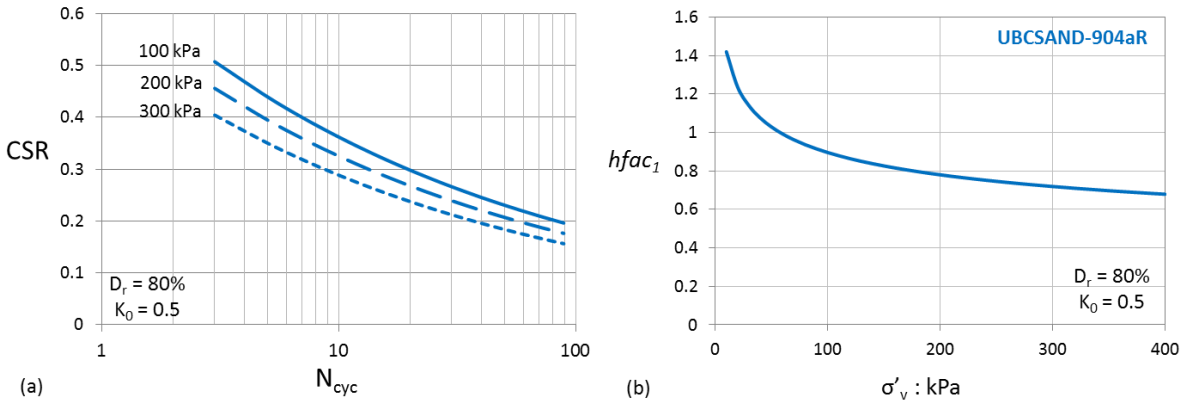

Figure 6. (a) Cyclic stress ratios versus number of equivalent uniform loading cycles in undrained direct simple shear loading to cause r_u=98% for D_r = 80% and varying vertical effective stress. (b) Corresponding values of $hfac_1$ parameter of UBCSAND-904aR (in FLAC).

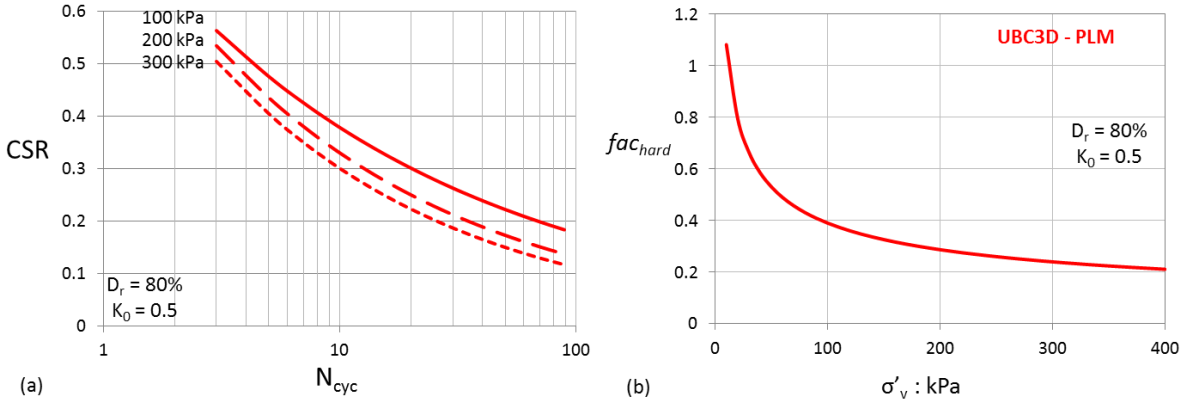

Figure 7. (a) Cyclic stress ratios versus number of equivalent uniform loading cycles in undrained direct simple shear loading to cause ru=98% for Dr = 80% and varying vertical effective stress. (b) Corresponding values of fac_{hard} parameter of UBC3D-PLM (in PLAXIS).

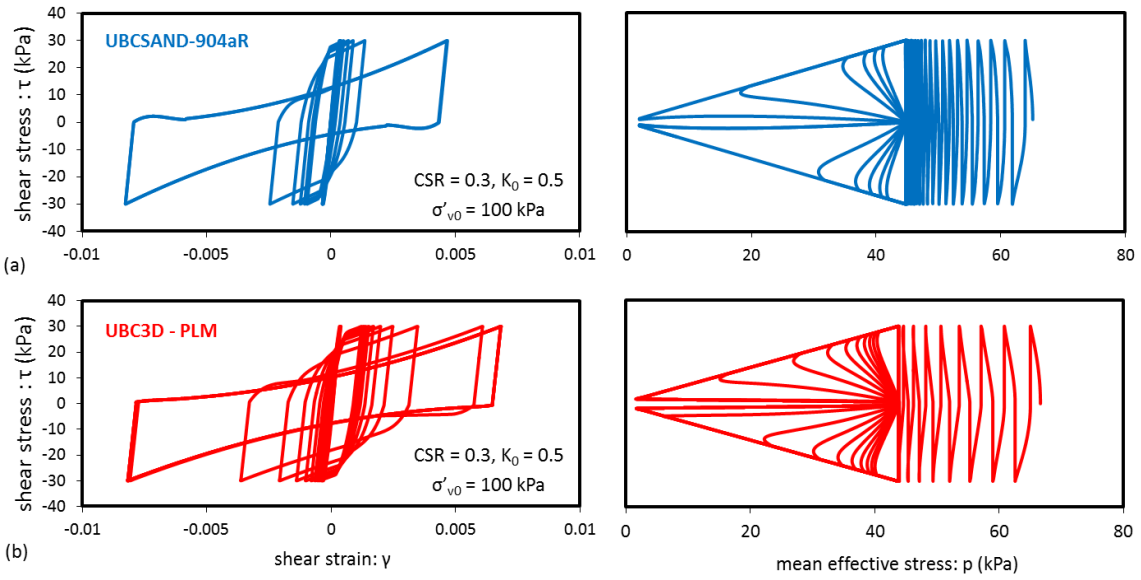

Figure 8. Simulated cyclic direct simple shear tests with (a) UBCSAND-904aR (in FLAC) and (b) UBC3D-PLM (in PLAXIS) for D_r = 80%.

5 CLASS A PREDICTION: FLAC AND PLAXIS

Numerical predictions obtained from both FLAC and PLAXIS are shown in terms of time histories at the measurement locations shown in Figure 1. Initially, comparison of the developed deformation mechanism of the quay-wall-soil-container system is held in order to ensure that both models can successfully reproduce the outward quay-wall displacement and rotation, as has been observed in various case histories. Figure 9 confirms that both models produce similar deformed meshes after the end of shaking. The contours of horizontal displacements obtained from both models, illustrated in Figure 10, indicate that sliding at the base of the quay-wall prevailed against bearing capacity failure.

The numerical analyses provide similar results in terms of the quay-wall outward displacement and rotation, as well as the settlement at the backfill (see Figures 11 and 12). Both models predict a residual horizontal displacement of the quay-wall in the order of 22 cm and a residual rotation of 0.24 deg.

Acceleration time histories, shown in Figure 13, also compare well, apart from some high-frequency spikes in case of FLAC analysis. The inward accelerations are systematically larger than their outward (seaward) counterparts which appear to have been curtailed due to excessive sliding at the base of the wall. The absence of long period pulses in the accelerogram obtained at the backfill is a sign of either no or limited soil liquefaction occurrence.

However, both analyses predict positive excess pore pressure development at the backfill away from the quay-wall, close to the base of the model (see Figure 14). In particular, in case of PLAXIS, where totally undrained conditions apply and no flow (dissipation) is accounted for, there is a pore pressure build up close to liquefaction. On the other hand, analysis in FLAC allows for concurrent generation and dissipation of pore water pressure leading thus, to less positive excess pore water pressure development. In contrast to what happens in the backfill away from the quay-wall, negative excess pore pressures develop close to the wall-soil interface (point 11 in Figure 1) due to the outward displacement of the quay-wall, in agreement with previous studies ([6], [7]).

6 CONCLUSIONS

Class A predictions were presented for seismic centrifuge modeling of a multi-block gravity quay-wall supporting a dense backfill of D_r=*80%*. Numerical analyses were performed with two different codes: i) finite difference code FLAC (coupled flow effective stress analysis) and ii) finite element code PLAXIS (undrained effective stress analysis). The constitutive models used for soil behavior are extensions of the original elasto-plastic model, UBCSAND. The two versions were extensively calibrated in order to render them equivalent in terms of cyclic liquefaction resistance. The analyses provided results in remarkable agreement, especially for the quay-wall performance. In detail, both analyses predicted that the quay-wall moved seawards by 22 cm at the top and rotated 0.24 deg. Sliding at the base of the quay-wall was the predominant mechanism to induce outward quay-wall displacement.

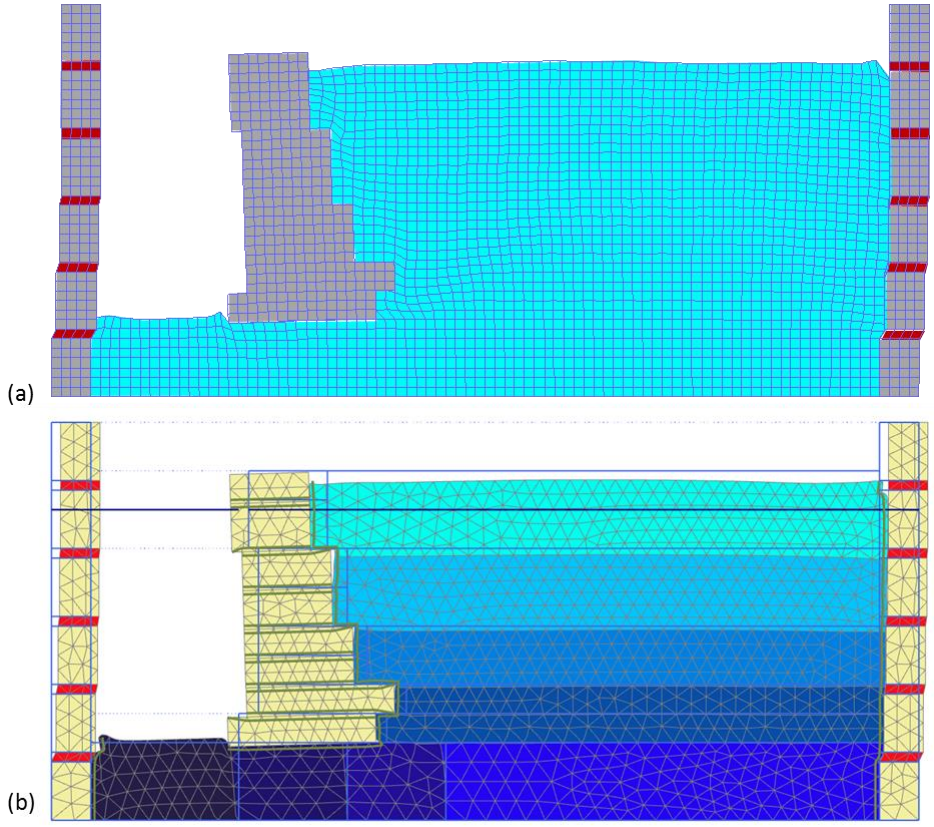

Figure 9. Deformed meshes after the end of shaking magnified 7 times: (a) FLAC and (b) PLAXIS.

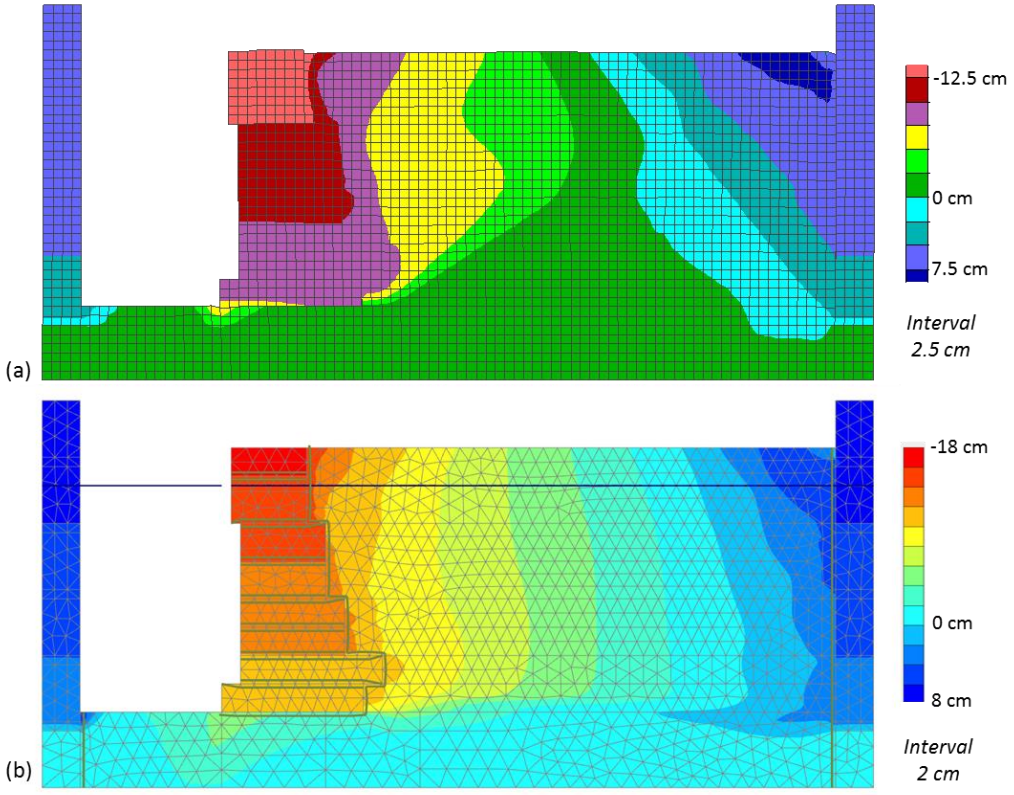

Figure 10. Contours of horizontal displacements after the end of shaking: (a) FLAC and (b) PLAXIS.

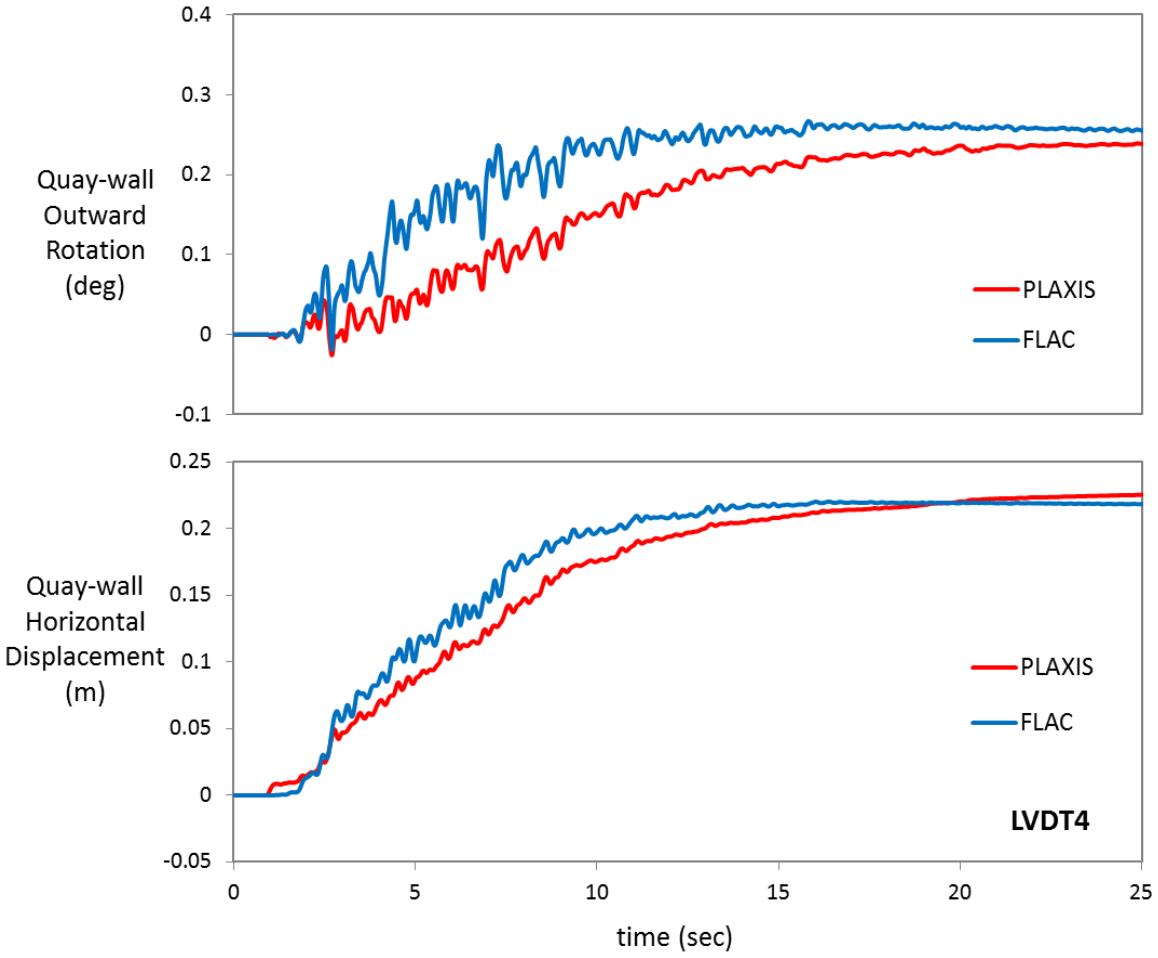

Figure 11. Predicted quay-wall rotation (top) and horizontal displacement at top (bottom).

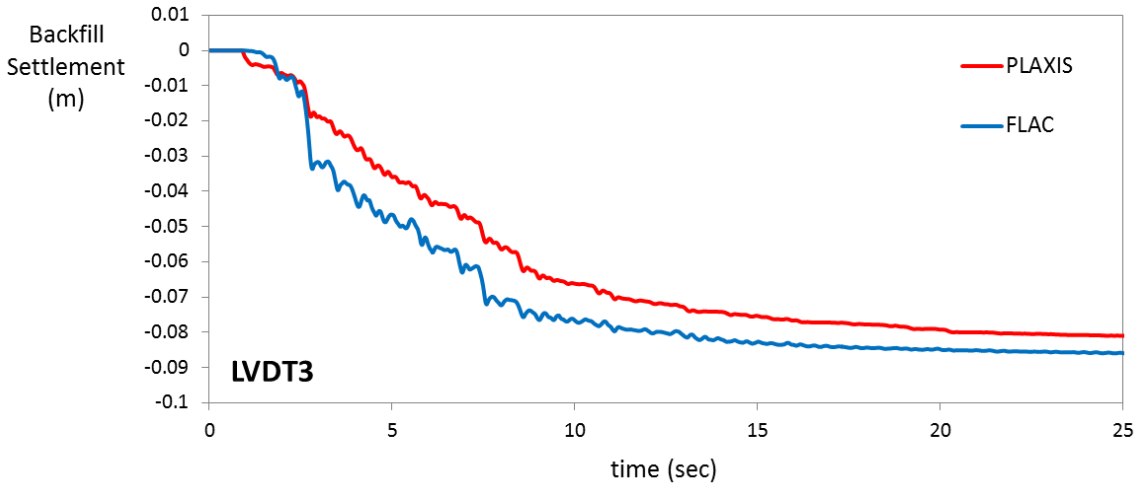

Figure 12. Predicted settlement of the backfill at location LVDT3 in Figure 1.

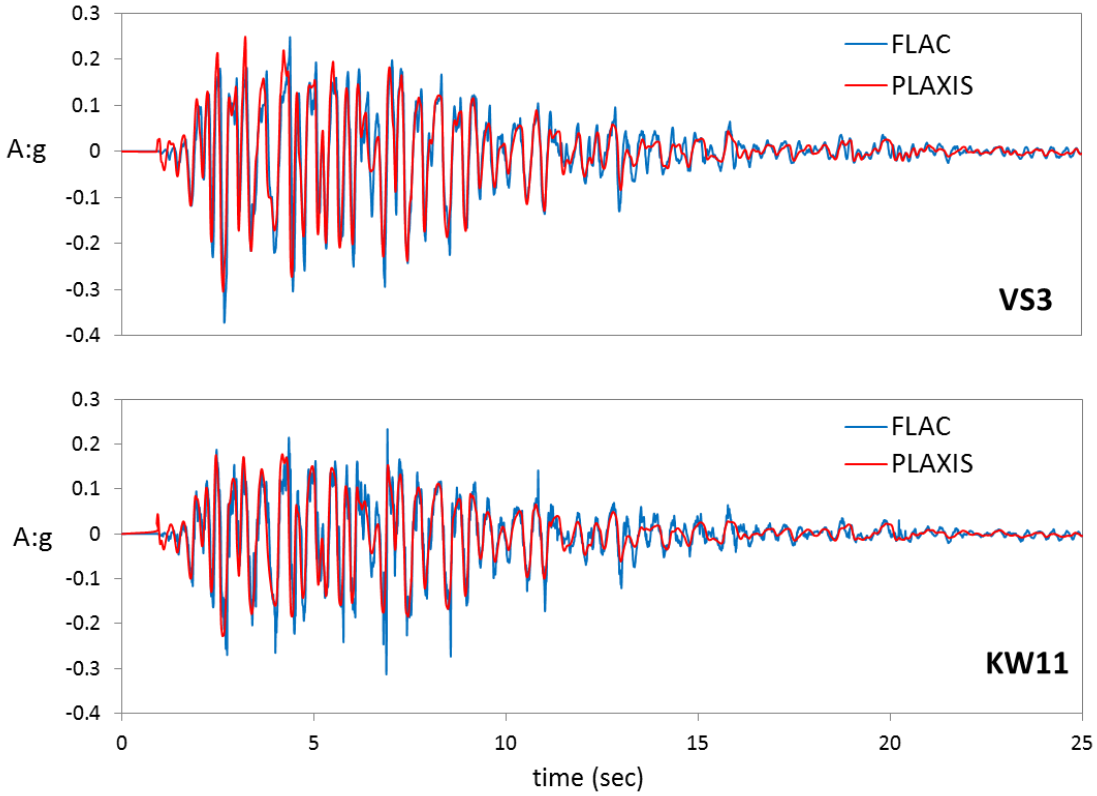

Figure 13. Predicted acceleration time histories at the top block of the quay-wall (top) and at the backfill 2m below to surface (bottom).

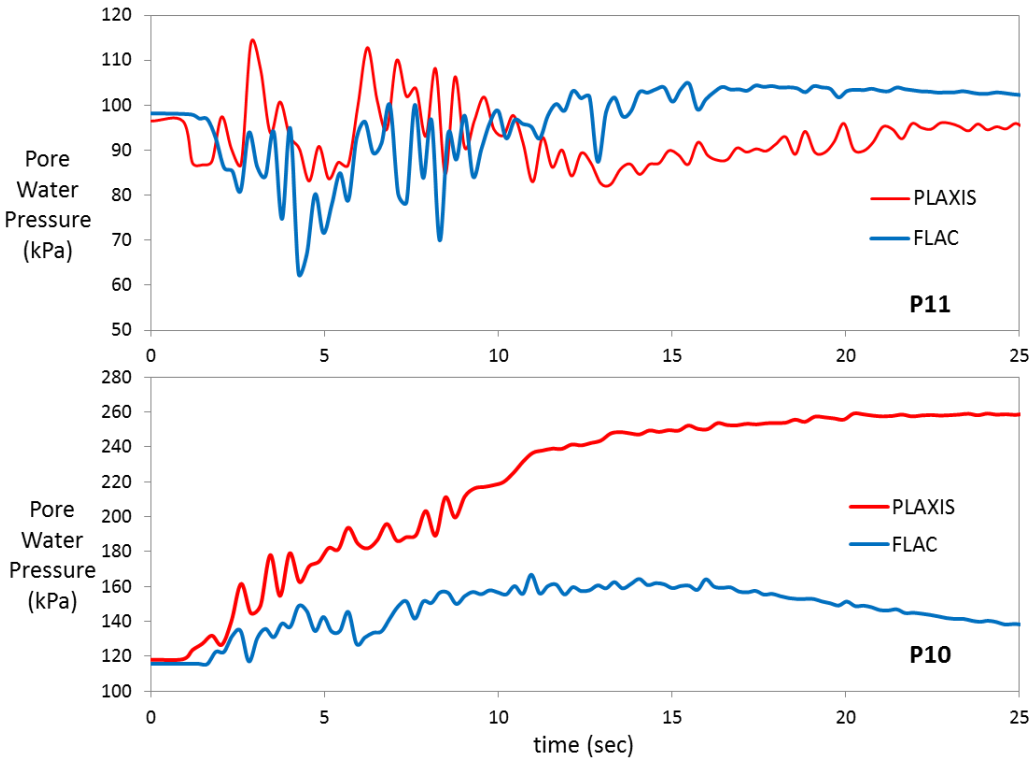

Figure 14. Predicted pore water pressures at locations shown in Figure 1.

ACKNOWLEDGEMENT

This research has been co-financed by the European Union (European Social Fund – ESF) and Greek national funds through the Operational Program "Education and Lifelong Learning" of the National Strategic Reference Framework (NSRF) - Research Funding Program: Thales. Investing in knowledge society through the European Social Fund, Project ID "UPGRADE".

REFERENCES

[1] Pitilakis K. and Moutsakis A., Seismic analysis and behaviour of gravity retaining walls – the case of Kalamata harbour quaywall. *Soil and Foundations*, **29**(1), 1-17, 1989.

[2] Egan J.A., Hayden R.F., Scheibel. L.L., Otus M., Serventi G.M., Seismic repair at Seventh Street Marine Terminal. *Grouting Soil Improvement and Geosynthetics, Geotechnical Special Publication, ASCE*, **30**, 867-878, 1992.

[3] Iai S., Matsunaga Y., Morita T., Miyata M., Sakurai H., Oishi H., Ogura H., Ando Y., Tanaka Y., Kato M., Effects of remedial measures against liquefaction at 1993 Kushiro – Oki earthquake. *Proc. Fifth U.S. – Japan Workshop on Earthquake resistant design of Lifeline Facilities and Countermeasures against Soil Liquefaction*, National Center for Earthquake Engineering Research, NCEER-94-0026, 135-152, 1994.

[4] Sugano T., and Iai S., *Damage to port facilities*. The 1999 Kocaeli Earthquake Turkey – Investigation into Damage to Civil Engineering Structures, Earthquake Engineering Committee, Japan Society of Civil Engineers, 6-1 – 6-14, 1999.

[5] Zarzouras O., Gerolymos N., Gazetas G., Seismic Response of Caisson Quay-Wall in a Liquefied Environment. Analysis of a Case History. *Proc. of the 6th Hellenic Conference on Geotechnical and Geoenvironmental Engineering*, Vol. 1, 549–556, Volos, Greece, September 29–October 1, 2010.

[6] Tasiopoulou P., Gerolymos N., Tazoh T. and Gazetas G., Pile-Group Response to Large Soil Displacements and Liquefaction: Centrifuge Experiments Versus a Physically Simplified Analysis. *Journal of Geotechnical and Geoenvironmental Engineering, ASCE* , **139**(2), 223-233, 2013.

[7] Tasiopoulou P., Gerolymos N, Gazetas G., Seismic Effective Stress Analysis of Gravity Block-Type Quay Walls: Application to Piraeus Port. *2nd European Conference on Earthquake Engineering and Seismology*, Istanbul, Turkey, 24-29 August, 2014.

[8] Inagaki H., Iai S., Sugano T., Yamazaki H. and Inatomi T., Performance of caisson type quay walls at Kobe port. *Soils and Foundations*, Special Issue on Geotechnical Aspects of the January 17 1995 Hyogoken-Nambu Earthquake, 119-136, 1996.

[9] Anastasopoulos I., Loli M., Antoniou M., Knappet J., Brennan A., Centrifuge testing of multi-block quay walls. *SECED 2015 Conference: Earthquake Risk and Engineering towards a Resilient World*, Cambridge UK, 9-10 July 2015.

[10] Itasca, *Fast Lagrangian Analysis of Continua*, Itasca Consulting Group Inc., Minneapolis, Minnesota, 2005.

[11] Puebla H., Byrne P.M. and Phillips R. Analysis of CANLEX Liquefaction Embankments: Prototype and Centrifuge Models. *Canadian Geotechnical Journal*, **34**(5), 641-657, 1997.

[12] Beaty M. and Byrne P., An effective stress model for predicting liquefaction behaviour of sand. *Geotechnical Earthquake Engineering and Soil Dynamics III*, *ASCE Geotechnical Special Publication*, **75**, 766-777, 1998

[13] Beaty M. and Byrne P., *UBCSAND constitutive model, Version 904aR*. Documentation Report: UBCSAND constitutive model on Itasca UDM Web Site, 2011.

[14] Galavi V., Petalas A. and Brinkgreve R.B.J, Finite element modeling of seismic liquefaction in soils. *Geotechnical Engineering Journal of the SEAGS & AGSSEA*, **44**(3), 55-64, 2013.

[15] Zienkiewicz, O.C., Bicanic N. and Shen F.Q., Earthquake input definition and the transmitting boundary conditions. *Proceedings of Advances in Computational Nonlinear Mechanics I*, Doltsinis (eds), Springer-Verlag, 109-138, 1988.

[16] Gerolymos N., Giannakou A., Anastasopoulos I., Gazetas G., Evidence of Beneficial Role of Inclined Piles: Observations and Summary of Numerical Analyses. *Bulletin of Earthquake Engineering*, **6**(4), 705-722, 2008.

[17] Zafeirakos A. and Gerolymos N., On the Seismic Response of Under-Designed Caisson Foundations. *Bulletin of Earthquake Engineering*, **11**(5), 1337-1372, 2013.

[18] Idriss, I. M. and Boulanger, R. W., *Soil liquefaction during earthquakes*, Monograph MNO-12, Earthquake Engineering Research Institute, Oakland, CA, 2008.

[19] Kammerer J W., Riemer M., Pestana J. and Seed R., A new mult-directional direct simple shear testing database. *13th World Conference on Earthquake Engineering*, Vancouver, B.C., Canada, Paper No. 2083, August 1-6, 2004.

[20] Sriskandakumar, S., *Cyclic loading response of fraser sand for validation of numerical models simulating centrifuge tests*. Master's thesis. The University of British Columbia, Department of Civil Engineering, 2004.

[21] Tatsuoka F., Ochi K., Fujii, S. and Okamoto, M., Cyclic triaxial and torsional strength of sands for different preparation methods. *Soils and Foundations*, **26**(3), 23-41, 1986.

[22] Tasiopoulou, P. and Gerolymos, N., Development of a modified elastoplasticity model for sand. *Proceedings of the Second International Conference on Performance–Based Design in Earthquake Geotechnical Engineering*, Taormina (Italy), 28-30 May, 2012.